NeuroImage: Clinical 32 (2021) 102874

Contents lists available at ScienceDirect

NeuroImage: Clinical

journal homepage: www.elsevier.com/locate/ynicl

Fusion analysis of gray matter and white matter in subjective cognitive decline and mild cognitive impairment by multimodal CCA-joint ICA

Lingyan Liang [a,1], Zaili Chen [b,c,1], Yichen Wei [d,1], Fei Tang [b,c], Xiucheng Nong [e], Chong Li [e], Bihan Yu [e], Gaoxiong Duan [a], Jiahui Su [e], Wei Mai [e], Lihua Zhao [e], Zhiguo Zhang [b,f,g,*], Demao Deng [a,*]

[a] The People's Hospital of Guangxi Zhuang Autonomous Region, Nanning 530021, Guangxi, China
[b] School of Biomedical Engineering, Health Science Center, Shenzhen University, Shenzhen 518060, China
[c] Department of Medical Instrument Measurement, Shenzhen Academy of Metrology and Quality Inspection, Shenzhen 518055, China
[d] Department of Radiology, First Affiliated Hospital, Guangxi University of Chinese Medicine, Nanning 530023, Guangxi, China
[e] Department of Acupuncture, First Affiliated Hospital, Guangxi University of Chinese Medicine, Nanning 530023, Guangxi, China
[f] Guangdong Provincial Key Laboratory of Biomedical Measurements and Ultrasound Imaging, Shenzhen 518060, China
[g] Peng Cheng Laboratory, Shenzhen 518055, China

ARTICLE INFO

Keywords:
Fusion analysis
Structural magnetic resonance imaging
Diffusion tensor imaging
Subjective cognitive decline
Mild cognitive impairment

ABSTRACT

Background: Previous multimodal neuroimaging studies analyzed each dataset independently in subjective cognitive decline (SCD) and mild cognitive impairment (MCI), missing the cross-information. Multi-modal fusion analysis can provide more integral and comprehensive information regarding the brain. There has been a paucity of research on fusion analysis of sMRI and DTI in SCD and MCI.

Materials and Methods: In the present study, we conducted fusion analysis of structural MRI and DTI by applying multimodal canonical correlation analysis with joint independent component analysis (mCCA-jICA) to capture the cross-information of gray matter (GM) and white matter (WM) in 62 SCD patients, 99 MCI patients, and 70 healthy controls (HCs). We further analyzed correlations between the mixing coefficients of mCCA-jICA and neuropsychological scores among the three groups.

Results: A set of joint-discriminative independent components of GM and fractional anisotropy (FA) exhibited significant links between SCD and HCs, as well as between MCI and HCs. The covariant abnormalities primarily involved the frontal lobe/middle temporal gyrus/calcarine sulcus-anterior thalamic radiation/superior longitudinal fasciculus in SCD, and middle temporal gyrus/ fusiform gyrus/caudate necleus-forceps minor/anterior thalamic radiation in MCI. There was no significant difference between SCD and MCI groups.

Conclusions: The covariant GM-WM abnormalities in SCD and MCI were found in specific brain regions involved in cognitive processing, which confirms the simultaneous GM and WM changes underlying cognitive decline. These findings suggest that multimodal fusion analysis allows for a more comprehensive understanding of the association among different types of brain tissues and its crucial role in the neuropathological mechanism of SCD and MCI.

Abbreviations: AAL, Automated Anatomical Labeling; AD, Alzheimer's disease; AFT, Animal Fluency Test; ANOVA, Analysis of variance; AVLT-dr, Auditory Verbal Learning Test delayed recall; BET, Brain Extraction Tool; CDR, Clinical Dementia Scale; BNT, Boston Naming Test; CSF, cerebrospinal fluid; DARTEL, diffeomorphic anatomical registration using exponentiated lie algebra; DMN, default mode network; DTI, diffusion tensor imaging; FA, fractional anisotropy; FDT, FMRIB's Diffusion Toolbox; FSL, FMRIB Software Library; FWHM, full-width at half-maximum; GDS, Geriatric Depression Scale; GM, gray matter; HC, healthy control; mCCA-jICA, multimodal canonical correlation analysis with joint independent component analysis; MAP, maximum a posteriori; MCI, mild cognitive impairment; MDL, minimum description length; MTL, medial temporal lobe; MMSE, Mini-Mental State Examination; MNI, Montreal Neurological Institute; MoCA, Montreal Cognitive Assessment; NIA/AA, National Institute on Aging/Alzheimer's Association; PVE, partial volume estimations; SCD, subjective cognitive decline; STT-A, Part A of Trail Making Test; STT-B, Part B of Trail Making Test; SVD, singular value decomposition; WM, white matter.

* Corresponding authors at: School of Biomedical Engineering, Health Science Center, Shenzhen University, Shenzhen 518060, China (Z. Zhang) ; The People's Hospital of Guangxi Zhuang Autonomous Region, Nanning 530021, Guangxi, China (D. Deng).

E-mail addresses: chenzaili2020@email.szu.edu.cn (Z. Chen), tangfei2017@email.szu.edu.cn (F. Tang), zgzhang@szu.edu.cn (Z. Zhang), demaodeng@163.com (D. Deng).

[1] Lingyan Liang, Zaili Chen and Yichen Wei have contributed equally to this work.

https://doi.org/10.1016/j.nicl.2021.102874
Received 15 April 2021; Received in revised form 30 October 2021; Accepted 1 November 2021
Available online 6 November 2021

1. Introduction

Subjective cognitive decline (SCD) has been proposed to represent a transitional stage to AD according to the National Institute on Aging/Alzheimer's Association (NIA/AA), and it is thought to be an intermediate stage between healthy controls (HCs) and individuals with mild cognitive decline (MCI) (Jessen et al., 2020). Previous neuroimaging studies revealed that the brain changes of SCD were intermediate between MCI and HC (Wang et al., 2012; López-Sanz et al., 2017; Lazarou et al., 2019). Increasing studies were focus on the neuroimaging of SCD with the aim of the identification of underlying pathological changes, but the results remain controversial. A growing number of multimodel neuroimaging studies have provided more complete understanding of the disease, while there is still a lack of consensus on the relationship of SCD and AD neuroimaging biomarkers. Previous studies using multimodel brain imaging analyzed each dataset independently, resulting in the loss of cross-information between imaging modalities. Multi-modal fusion analysis may directly and reliably reveal underlying interrelationships of changes in each modality, and provide more integral and comprehensive information regarding the brain. It is favorable to be applied for the detection of complicated and potentially weak effects which are hidden in a high-dimensional data sets(Calhoun and Sui, 2016). Thus, multi-modal fusion analysis may help to better elucidate the pathophysiological mechanisms of the disease, and provide relevant imaging biomarkers. Furthermore, it can provide robustness to noise (Calhoun and Sui, 2016). Sui *et al.* (Sui et al., 2013b) has proposed a data fusion model—namely multimodal canonical correlation analysis with joint independent component analysis (mCCA-jICA)—which synthesizes and complements the specific advantages of each modality and has potential to uncover associations among abnormalities found in multiple modalities. The mCCA-jICA is a data-driven multivariate fusion method that can obtain the interaction between different imaging modalities and cross-modal joint information (Sui et al., 2011; Sui et al., 2014). More precisely, mCCA is first used to find maximally correlated components between multiple modalities, and then jICA is used to decompose these correlated components into spatially independent components (ICs), which are concatenated spatial maps of different modalities. In other word, the spatial maps of different modalities in one IC are correlated between modalities, while spatial maps of different ICs are independent with each other. A previous study conducted multimodal fusion analysis using mCCA-jICA and found results supporting and extending previous findings derived from single modality analyses, and also provided a more comprehensive understanding of the underlying relationship between functional and structural abnormalities in schizophrenia (Lottman et al., 2018). Furthermore, these selected group-discriminating components might be useful for diagnosing schizophrenia (Sui et al., 2013a; Yang et al., 2010). Additionally, Ouyang *et al.* (Ouyang et al., 2015) applied fusion analysis to GM and WM data in AD to demonstrate the reliability of the results, and expanded our knowledge of neuropathological mechanisms from the perspective of covariate patterns in AD.

To the best of our knowledge, there has been a paucity of research on fusion analysis of sMRI and DTI in SCD and MCI. We hypothesized that there exist covariant GM-WM abnormalities in SCD and MCI, and these covariant GM-WM abnormalities are associated with cognitive performance. In the present study, we fused abnormalities in GM and fractional anisotropy (FA) via mCCA-jICA to investigate the covariate pattern of GM and WM in SCD and MCI as well as the correlation between the mixing coefficients and the cognitive assessments.

2. Materials and methods

2.1. Participants

Sixty-two SCD and 99 MCI patients as well as 70 HCs matched with the patients by age, gender, and years of education were enrolled in the present study. All participants were recruited from the First Affiliated Hospital of Guangxi University of Chinese Medicine and its Renai Branch Hospital, as well as from several aged-community activity centers in Nanning, Guangxi Province. All participants signed an informed consent prior to enrollment. This study was permitted by the Medicine Ethics Committee of First Affiliated Hospital of Guangxi University of Chinese Medicine.

The inclusion criteria for patients were as follows: (1) aged 55–75 years; (2) right-handed; (3) self-reported changes in cognition; (4) unaffected daily life activities and occupation. Exclusion criteria for patients with MCI or SCD were as follows: (1) advanced, severe, or unstable diseases such as liver, kidney, and other serious primary diseases; (2) severe hearing and/or visual impairment; (3) dementia, cerebral infarction, or any physical or mental illness that can cause brain dysfunction; (4) taking drugs that may cause cognitive changes or important organ failure (e.g., heart, brain, and kidney) prior to the experiment; (5) did not meet requirements for undergoing MRI scanning, such as patients with claustrophobia, metal dentures, or other metal implants that could not be removed. The diagnostic criteria for MCI (Albert et al., 2011) was as follows: (1) self-reported memory loss that was confirmed by an informed individual; (2) relatively intact or only slightly damaged other cognitive functions; (3) daily life activities not affected; (4) did not reach the diagnostic criteria for dementia; (5) Clinical Dementia Scale (CDR) score was 0.5, the Mini-Mental State Examination (MMSE) (Folstein et al., 1975) score was 24–27, the Montreal Cognitive Assessment (MoCA) (Nasreddine et al., 2005) score was < 26; and the Global Deterioration Scale (GDS) score was 2–3. Then, participants with a normal objective performance level(the MMSE score > 27, MoCA score ≥ 26, the CDR score $= 0$, and the GDS score $= 1$) underwent the following six tests in three cognitive domains: Auditory Verbal Learning Test (AVLT delayed recall and AVLT-recognized) for memory, Animal Fluency Test (AFT) and 30-item Boston Naming Test (BNT) for language, and Part A (STT-A) and Part B (STT-B) of Trail Making Test for executive functions. Participants were excluded if each of the three cognitive domains had an impaired score [defined as > 1 standard deviation(SD)]; or if abnormalities occurred on two measures in the same cognitive domain, defined as > 1 SD (Edmonds et al., 2015). Next, individuals with complaints of memory decline were regarded as the SCD group (Jessen et al., 2014), whereas individuals without complaints and whose cognitive functions passed neuropsychological tests were included in the HC group. The demographic information of all participants is shown in Table 1.

2.2. Data acquisition

All MRI data were acquired by a 3.0-Tesla Siemens Magnetom Verio scanner (Siemens Medical, Erlangen, Germany). A Siemens standard EPI function head coil was utilized to reduce head movement. High-resolution structural images were collected with a volumetric three-dimensional spoiled gradient recall sequence with the following parameters: TR/TE $=$ 1900/2.22 ms, field of view (FOV) $=$ 250 $\times$ 250 mm^2, matrix size $=$ 256 $\times$ 256, flip angle $= 9°$, slice number $=$ 168, and voxel size $= 0.98 \times 0.98 \times 1\ mm^3$. DTI data were obtained with a single-shot, echo-planar imaging sequence. The diffusion sensitizing gradients

Table 1
Demographic information of all participants.

Demographic variable	HC (n = 70)	SCD (n = 62)	MCI (n = 99)
Age (mean ± SD, years)	64.64 ± 5.76	64.85 ± 5.62	65.11 ± 6.55
Gender (female/male)	44/ 26	42/ 20	71/ 28
MMSE	29.13 ± 0.74	28.89 ± 0.85	25.85 ± 1.03
MoCA	26.11 ± 2.01	24.85 ± 2.49	21.36 ± 3.0

Note: HC: healthy control; SCD: subjective cognitive decline; MCI: mild cognitive impairment; MMSE: Mini-Mental State Examination; MoCA: Montreal Cognitive Assessment

were applied along 30 noncollinear directions (b = 1000 s/mm2) with an acquisition without diffusion weighting (b = 0 s/mm^2). The imaging parameters were 45 contiguous axial slices with a slice thickness of 3 mm, TR = 6800 ms, TE = 93 ms, data matrix of 128 × 128, and FOV of 240 × 240 mm^2.

2.3. Data analysis

2.3.1. Preprocessing and feature extraction

The sMRI data were preprocessed using the VBM Toolbox (http://dbm.neuro.uni-jena.de/vbm) in Statistical Parametric Mapping (SPM12, https://www.fil.ion.ucl.ac.uk/spm/software/spm12/). In the VBM analysis, we obtained the average template (i.e., the mask) from the images of all subjects so that the GM extracted from original data can register into the Montreal Neurological Institute (MNI) space. First, each participant's MRI data was segmented into GM, WM and cerebrospinal fluid (CSF) images using adaptive maximum a posteriori (MAP) (Rajapakse et al., 1997) and partial volume estimations (PVE) (Tohka et al., 2004). Next, the DARTEL (Ashburner, 2007) algorithm was used to create the GM average template of all individuals and then each individual's GM images were registered to the average template. After registration, the normalized GM images were multiplied by the nonlinearly deformed Jacobian determinant to preserve the absolute volumes of GM in each individual's native space. The dimension of the template and all registered GM images is 121 × 145 × 121. Finally, all GM images were smoothed with an 8-mm full-width at half-maximum (FWHM) Gaussian kernel.

DTI images were analyzed via the FMRIB Software Library (FSL) (https://fsl.fmrib.ox.ac.uk/fsl). For the diffusion-weighted images of each participant, the eddy currents and head motions were corrected to the non-diffusion-weighted images in the FMRIB's Diffusion Toolbox (FDT) 2.0. Then the volumes without diffusion weighted (b0 images) were averaged and the non-brain tissues of b0 images were discarded using the Brain Extraction Tool (BET). FA maps were generated based on the diffusion tensors reconstructed with the DTIfit program. Next, the TBSS (Smith et al., 2006) was performed on all participants' FA images to obtain the FA skeleton images. Firstly, the FA image of each participant was nonlinearly normalized to the MNI space. Then the mean FA image was calculated and the mean FA skeleton image was created with the threshold at FA > 0.2. Subsequently, the FA image aligned by each subject was projected onto the mean FA skeleton image by calculating the maximum FA values from the nearest tract center and filling the corresponding position in the skeleton. Finally, all subjects' skeletonized FA images were calculated in the standard 1 × 1 × 1 mm^3 MNI space, and smoothed with a 8-mm FWHM Gaussian kernel. The dimensionality of FA data was 182 × 218 × 182.

2.3.2. Multimodal CCA- joint ICA

To reduce the redundancy of high-dimensional MRI data, the features of either modality (GMV for sMRI and FA for DTI) were extracted after preprocessing and were then fused by the mCCA-jICA method. Here, features were a subset of variables extracted from one imaging modality (GMV from sMRI and FA from DTI), which were measures of structural abnormalities in GM and WM of the brain (Calhoun and Adali, 2008).

The fusion analysis of mCCA-jICA was performed with the Fusion ICA Toolbox (FITv2.0d, http://mialab.mrn.org/software/fit/). Fig. 1 shows a flowchart of mCCA-jICA. Following feature extraction, features of two modalities, GMV and FA were reshaped into feature matrices X_1 and X_2 respectively, and the dimensionality of both X_1 and X_2 was [number of participants] × [number of voxels]. Each row of a feature matrix represents a stacked 3D map of a participant. Next, both feature matrices were normalized to z-scores so that they have the same sum-of-squares (computed across all participants and all voxels). Normalization was necessary because GM and FA data have largely different ranges (Sui et al., 2011). After normalization, a minimum description length (MDL) criterion was used to estimate the number of ICs for either dataset (Li et al., 2007) and dimensionality reduction of the feature matrices was performed using singular value decomposition (SVD). More precisely, the SVD of an $m \times n$ matrix M is a factorization of the form $U\Sigma V^*$, where U is an $m \times m$ unitary matrix, Σ is an $m \times n$ rectangular diagonal matrix with non-negative real numbers on the diagonal (singular values), and V is an $n \times n$ unitary matrix. The columns of U are the left-singular vectors of M, and the columns of V are the right-singular vectors of M. The singular values in the diagonal matrix Σ can be used to understand the amount of variance explained by each of the singular vectors. Therefore, we can limit the number of vectors (features) to the amount of variance we wish to capture, and reducing the number of vectors can help eliminate noise in the original data set. More details about SVD and its applications on dimensionality reduction can be found in any classical book about statistical learning or matrix computation, such as (Strang, 1993). The number of features to be retained by SVD was determined by the scree plot in the FIT toolbox. Next, mCCA was performed on the dimensionally-reduced matrices to obtain the canonical variant matrix, $[\ B_1\ ,\ B_2\ ]$, and the associated component matrix, $[\ C_1\ ,\ C_2\ ]$, for either modality. Subsequently, the jICA algorithm was applied to the associated component matrix, $[C_1, C_2]$, to obtain the maximized joint-independence component matrix, $[S_1, S_2]$, and the mixing coefficient matrix, D. The final mixing coefficient matrix, $[\ A_1\ ,\ A_2\ ]$, was calculated by obtaining the product of the canonical variant matrix and the mixing coefficient matrix of the jICA (B_1, D for GM; B_2, D for FA), which represent the source differences between the SCD and HC groups for either modality. The columns of the resulting matrices represent the weights from each IC. Thus, the final mixing coefficient matrix, $[A_1\ ,\ A_2\ ]$, and its corresponding sources contain both shared and unique information across modalities. The outputs of the mCCA-jICA fusion are joint ICs and the corresponding mixing coefficients. One joint IC (one row of $[S_1,S_2]$) consists of a spatial map of GMV (one row of S_1) and a spatial map of FA (one row of S_2), which represent the GMV or FA values of all voxels or vertexes of this IC. The mixing coefficient of each IC and each individual indicates how much of the IC is required to reconstruct the individual's source data (A_1 for GMV and A_2 for FA) (Lerman-Sinkoff et al., 2017). The group discriminant components can be obtained by comparing the mixing coefficients of each modality so that the brain's spatial maps (GMV or FA) with significant between-group difference can be found.

2.3.3. Statistics inference of mixing coefficients

We first used the Kolmogorov-Smirnov test to examine the normality of mixing coefficients (A_1 and A_2) to be compared among groups (HC vs. SCD, HC vs. MCI, SCD vs. MCI). We found that the mixing coefficients of all sMRI joint components were normally distributed but most of the mixing coefficients of DTI joint components were not normally distributed (see Supplementary Table 1 and Supplementary Figs. 1 and 2 for details). Because sMRI_GMV and DTI_FA have different statistical distributions, we applied different statistical tests in the revised manuscript. More precisely, we used one-way ANOVA on the mixing coefficients of sMRI_GMV and Kruskal-Wallis test (the nonparametric alternative to ANOVA) on the mixing coefficients of DTI_FA components. Both ANOVA and Kruskal-Wallis test were followed by post-hoc Tukey-Kramer test. Those components with significant group differences between the mixing coefficients of two groups are referred to as group-discriminative components. If statistical significance was reached for the same IC from both modalities, such a component was considered as a joint group-discriminative IC, which can differentiate groups in both sMRI and DTI. The significant sources (the row of the joint source matrix) were converted to Z-scores and then reshaped into 3D brain maps (GM regions and WM regions). Previous studies have shown that 2–3 is a reasonable range of Z-scores representing significantly-activated voxels (Sui et al., 2011; Kim et al., 2015; Ouyang et al., 2015; Yang et al., 2019). Here we set a threshold at $|Z| \geq 2$ to only show brain regions with

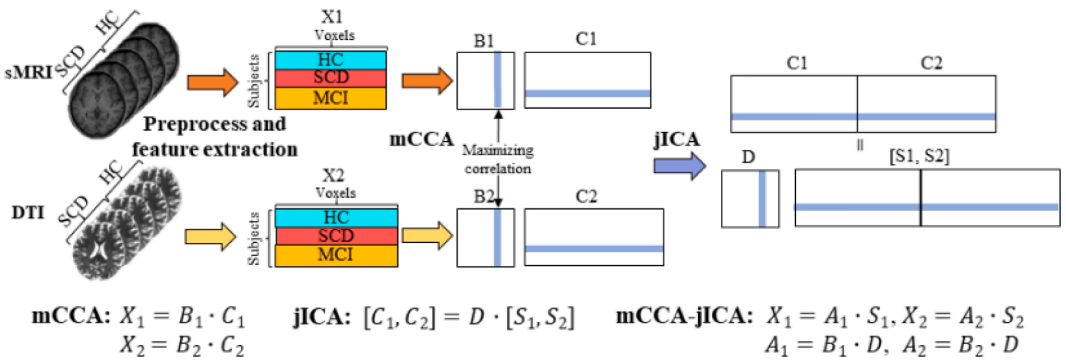

Fig. 1. Flowchart of mCCA-jICA for fusion analysis of sMRI and DTI images. Firstly, the features of two modalities (GMV for sMRI and FA for DTI) were extracted after pre-processing, and the GMV and FA features were reshaped into feature matrices X_1 and X_2 , respectively. After normalization and dimensionality reduction, mCCA was performed on X_1 and X_2 to obtain the canonical variants $[B_1, B_2]$ and the associated components $[C_1, C_2]$. Then jICA was applied to the associated component $[C_1, C_2]$ to obtain the maximized joint-independence component matrices $[S_1, S_2]$ and the mixing coefficient matrix D . The final mixing coefficient matrix A_1 and A_2 were calculated as $A_1 = B_1$•D (for GM V) and $A_2 = B_2$•D (for FA), while the original data matrices can be denoted as $X_1 = A_1$•S_1 and $X_2 = A_2$•S_2.

greater GMV/FA values in the 3D spatial map of each joint IC. For the results of GM, we used the Automated Anatomical Labeling (AAL) atlas (Tzourio-Mazoyer et al., 2002) to summarize the structures. For the results of WM, we used the Johns Hopkins University (JHU) white-matter tractography atlas in FSL to locate those group-discriminative regions. The ICs with the frames in the same color stand for joint ICs.

2.3.4. Correlation analysis between mixing coefficients and behavioral indexes

Correlation analysis was performed between the mixing coefficients of group discriminative ICs and behavioral indexes, including MMSE and MoCA. Specifically, we calculated the Pearson correlation coefficient between MMSE/MoCA and the mixing coefficients of group-discriminative ICs within either group, and then examined whether such a relationship was significantly different between any two groups. The p values with asterisk (*) passed FDR-corrected threshold of 0.05.

2.3.5. Correlation between mixing coefficients and cognitive performance in SCD

We performed correlation analysis between the mixing coefficients and measurements of six cognitive tests for three cognitive domains in SCD patients. These measurements from different cognitive tests were composed of delayed recall (AVLT-dr) and recognition of the AVLT, STT-A and STT-B, AFT, and the 30-item BNT.

3. Results

By using the mCCA-jICA method together with the MDL criterion, we identified in total 15 joint ICs, each of which is a concatenation of correlated GMV and FA features.

For a better understanding of the results, in the following we explain (1) what is a joint component, and (2) why a joint component may only have one modality showing significant difference between groups.

First, the outputs of the mCCA-jICA method are a series of joint ICs and the corresponding mixing coefficients. One joint IC consists of two parts: a vector of GMV features and a vector of FA features. These two types of features are concatenated together to form the joint IC and they are correlated with each other. Here, “joint” means these two types of features are correlated with each other and they are treated as a whole when performing joint independent component analysis (jICA). In another word, all ICs decomposed by mCCA-jICA were joint ICs. A “joint” IC means that features of two modalities are concatenated and are decomposed together, but it does not mean both modalities should have the same properties when performing between-group comparisons.

Second, the correlation between two modalities of one joint IC does not mean both modalities should show the same level of statistical difference between groups. Inter-group statistical tests were performed for each modality separately, because they were used to compare mixing coefficients, which have different values for different modalities. Hence, it is quite possible that one modality of a joint IC is different between two groups but the other modality of this joint IC is not different between two groups.

3.1. Group-discriminative independent components

By applying intergroup statistical analysis to the mixing coefficients of each component, three components of sMRI (IC01, IC05, and IC07) and one component of DTI (IC07) were identified as group discriminative components between HCs and SCD patients (Fig. 2). The regions in these identified ICs of sMRI mainly included the precentral gyrus, postcentral gyrus, middle frontal gyrus, and middle temporal gyrus, as well as DTI-identified regions consisting of the anterior thalamic radiation and superior longitudinal fasciculus. Meanwhile, six components of sMRI (IC01, IC03, IC04, IC05, IC07, and IC09) and one components of DTI (IC09) were found to be group-discriminative between HCs and MCI patients (Fig. 3). The main GM regions in these ICs included the thalamus, insula, precentral gyrus, inferior temporal gyrus, superior temporal gyrus, middle temporal gyrus, fusiform gyrus, middle frontal gyrus, precentral gyrus, caudate nucleus, hippocampus, and the *para*-hippocampal gyrus. In addition, the main discriminative FA tracts between HCs and MCI patients included the forceps minor, anterior thalamic radiation. Four sMRI components (IC04, IC06, IC07, and IC09) and one DTI components (IC03) were revealed to be group-discriminative between SCD and MCI patients (Fig. 4). Specifically, GMV changes existed mainly in the thalamus, hippocampus, fusiform gyrus, precentral gyrus, postcentral gyrus, superior frontal gyrus, superior temporal gyrus, middle temporal gyrus, and caudate nucleus. Furthermore, WM tracts mainly differed in the cingulate gyrus, cingulum (hippocampus), anterior thalamic radiation, inferior longitudinal fasciculus, superior longitudinal fasciculus, and corticospinal tract. The details of group-discriminative ICs are listed in Supplementary Tables 2 and 3. Additionally, correlations between mixing coefficient matrices (A1 and A2) for all the components are listed in Table 2. Importantly, these correlations can reveal latent covariant relationships across multiple morphological measurements. Take IC7 as an example. When comparing SCD and HC, GM_IC7 and FA_IC7 were group-discriminative components, which contained abnormal regions including the frontal lobe, middle temporal gyrus, and calcarine sulcus in sMRI, and the anterior thalamic radiation and superior longitudinal fasciculus in DTI. Because GM_IC7 and FA_IC7 are correlated ($p = 5.899 \times 10^{-5}$), we can infer the latent covariant relationship between GMV and FA as follows. The anterior thalamic radiation (as found by analysis

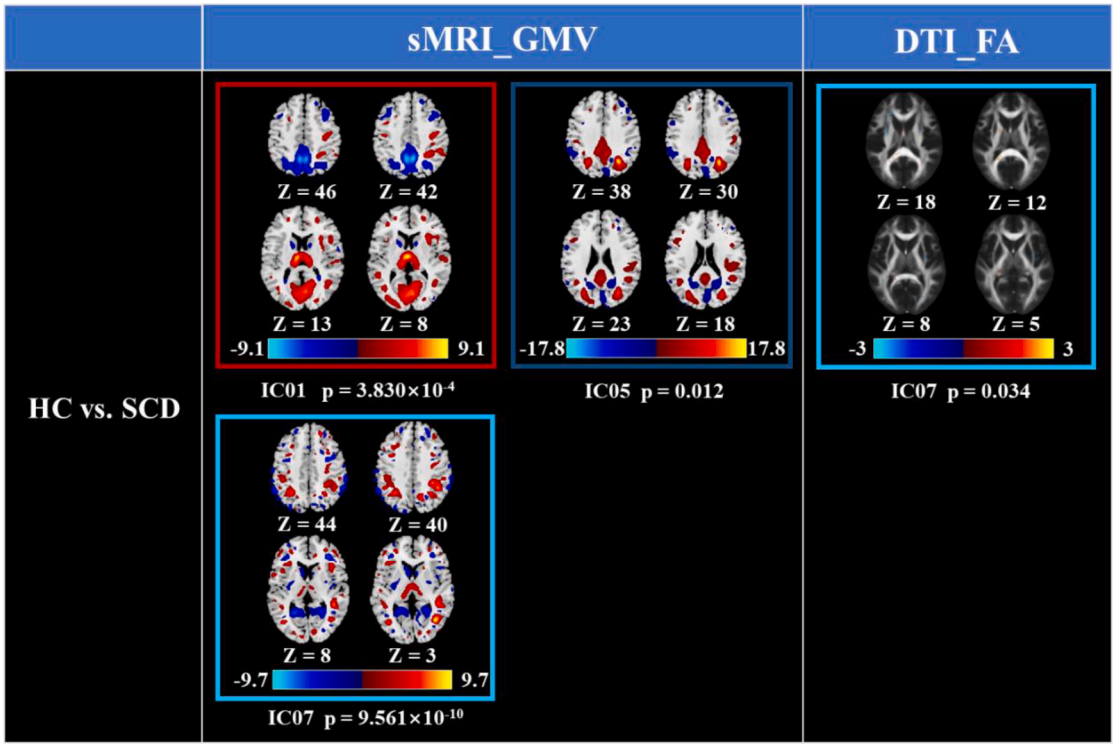

Fig. 2. Main group-discriminative ICs between HCs and SCD patients. GMV and FA were shown in coronal brain maps in terms of z-scores (positive: red, negative: blue; a threshold at $|Z| \geq 2$ was set for visualizing brain regions with large GMV or FA values). Those listed p-values were obtained by post-hoc Tukey-Kramer test between HC and SCD. If an IC was framed in the same color for sMRI_GMV and DTI_FA, it means both modalities of this IC were different between these two groups (IC07 in this figure). (For interpretation of the references to color in this figure legend, the reader is referred to the web version of this article.)

of DTI) connects the anterior and medial regions of the thalamus to the frontal lobe, and the superior longitudinal fasciculus projects from the frontal lobe to the temporal, parietal, and occipital lobes. The regions in the sMRI can be found to overlap with the regions connected by the anterior thalamic radiation and the superior longitudinal tract. These results indicate that GM changes in these regions may share a latent covariant relationship with FA abnormalities.

3.2. Correlation between IC mixing coefficients and behavioral indexes

For HCs and MCI patients, three ICs showed significant correlations between the mixing coefficients and MoCA (Fig. 5). Specifically, the mixing coefficients of GM_IC05 in MCI patients showed a significant positive correlation with the corresponding MoCA ($R = 0.258$, $^*p = 0.010$), while the mixing coefficients of this IC in HCs did not show a significant correlation with MoCA ($R = 0.062$, $p = 0.611$). The mixing coefficients of GM_IC05 in both HCs and MCI patients also showed a significant correlation with MoCA ($R = 0.317$, $^*p = 2.613 \times 10^{-5}$). For GM_IC07, the mixing coefficients in MCI patients showed a significant positive correlation with MoCA ($R = 0.251$, $^*p = 0.012$), whereas the mixing coefficients in HCs of this IC were not significantly correlated with MoCA ($R = 0.082$, $p = 0.498$). The mixing coefficients of GM_IC07 in both HCs and MCI patients showed a significant negative correlation with MoCA ($R = -0.325$, $^*p = 1.611 \times 10^{-5}$). As for GM_IC09, the mixing coefficients in HCs and MCI patients were not significantly positively correlated with MoCA (HCs: $R = -0.130$, $p = 0.282$, MCI patients: $R = -0.158$, $p = 0.119$), whereas the mixing coefficients of GM_IC09 in HCs and MCI patients were significantly negatively correlated with MoCA ($R = -0.563$, $^*p = 5.829 \times 10^{-14}$). No significant correlation was found between the mixing coefficients of group-discriminative ICs extracted from DTI and MoCA. There was no significant correlation between the group-discriminative mixing coefficients and MMSE for either HCs or MCI patients.

For SCD and MCI, two ICs were found to be significantly correlated between the mixing coefficients and MoCA (Fig. 6). Specifically, the mixing coefficients of GM_IC07 in MCI were significantly positively correlated with MoCA ($R = 0.251$, $^*p = 0.012$), while the mixing coefficients of this IC in SCD were not significantly correlated with MoCA ($R = -0.117$, $p = 0.367$). The mixing coefficients of GM_IC07 in SCD and MCI patients showed a significant positive correlation with MoCA ($R = 0.349$, $^*p = 5.669 \times 10^{-6}$). For GM_IC09, the mixing coefficients in the SCD and MCI groups were not significantly positively correlated with MoCA (SCD: $R = 0.223$, $p = 0.082$, MCI: $R = -0.158$, $p = 0.119$), but the mixing coefficients of GM_IC09 in SCD and MCI patients were significantly negatively correlated with MoCA ($R = -0.356$, $^*p = 3.587 \times 10^{-6}$). No significant correlation was found between the mixing coefficients of group-discriminative ICs extracted from DTI and MoCA. There was no significant correlation between the group-discriminative mixing coefficients for SCD, MCI, and MMSE.

3.3. Correlation between mixing coefficients and cognitive performance in SCD

For GM IC06, we found that the mixing coefficients in SCD patients were significantly correlated with AVLT-dr ($R = -0.332$, $p = 8.463 \times 10^{-3}$). For GM IC07, the mixing coefficients in SCD patients were significantly correlated with both STT-B ($R = -0.337$, $p = 7.350 \times 10^{-3}$) and AFT ($R = 0.330$, $p = 8.880 \times 10^{-3}$). As for WM IC06, a significant correlation was found between the mixing coefficients and AVLT-dr ($R = -0.330$, $p = 8.798 \times 10^{-3}$). Additionally, a significant correlation was found between the mixing coefficients of WM IC07 and AVLT-dr ($R = -0.329$, $p = 8.973 \times 10^{-3}$). Scatter plots corresponding to the above-mentioned mixing coefficients and measurements of cognitive tests are illustrated in Fig. 7.

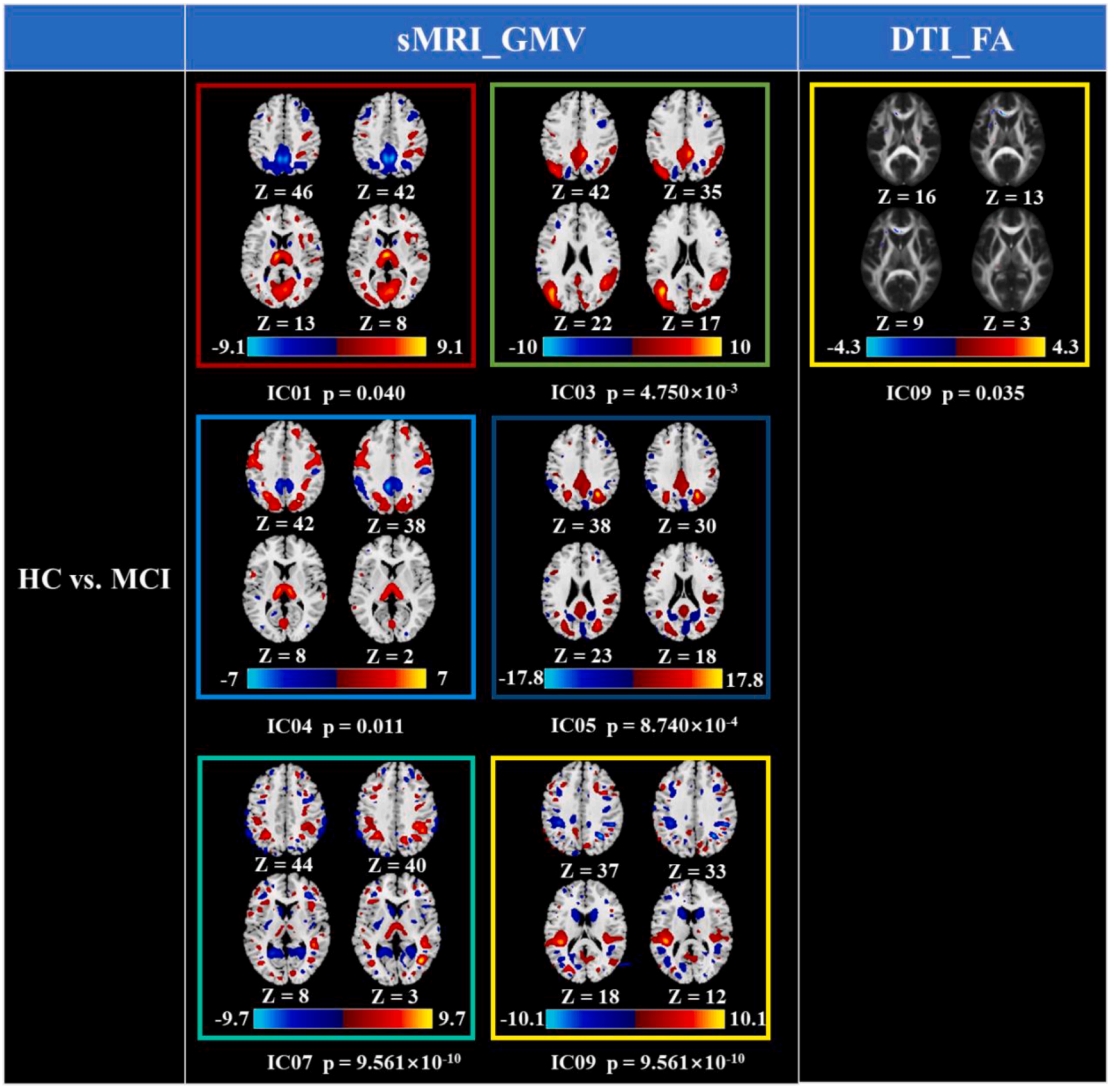

Fig. 3. Main group-discriminative ICs between HCs and MCI patients. GMV and FA were shown in coronal brain maps in terms of z-scores (positive: red, negative: blue; a threshold at $|Z| \geq 2$ was set for visualizing brain regions with large GMV or FA values). Those listed p-values were obtained by post-hoc Tukey-Kramer test between HC and MCI. If an IC was framed in the same color for sMRI-GMV and DTI_FA, it means both modalities of this IC were different between these two groups (IC09 in this figure). (For interpretation of the references to color in this figure legend, the reader is referred to the web version of this article.)

4. Discussion

In the present study, we performed fusion analysis of sMRI and DTI via mCCA + jICA among MCI patients, SCD patients, and HCs. The aim of our study was to identify the covariate changes of multimodal MRI and their correlations with cognition. We identified large-scale GM and changes in SCD and MCI patients. Particularly, we found one joint GM-WM component in either MCI or SCD, as compared to HC. In addition, the mixing coefficients of the joint GM-WM components were found to be significantly correlated with neuropsychological test scores in SCD patients. In the following, we mainly focus on discussion of group differences in covariation.

4.1. Methodological consideration

We first discussed several issues and considerations in the collection and analyses of multimodal MRI data.

4.1.1. Patient recruitment

One limitation of the present study is that the SCD and MCI groups were not tested for underlying AD pathology because of the lack of technology and equipment to get the information. In the present study, SCD and MCI were diagnosed according to the criteria proposed by the Subjective Cognitive Decline Initiative (SCD-I) Working Group (Jessen et al., 2014) and the National Institute on Aging Alzheimer's Association (NIA-AA) workgroups (Albert et al., 2011), in which SCD and MCI were considered due to AD. Therefore, we regarded SCD/MCI as pre-dementia states of AD in the present study in spite of the lack of tests for underlying AD pathology. However, these groups could be heterogeneous pathologically, which may influence our results. It is certain that the biomarker evidence for AD (such as aggregated Aß42/tau or associated pathologic state) and presence of the APOE ε4 genotype will increase the likelihood of preclinical AD in individuals with SCD or MCI.

4.1.2. MoCA and MMSE

Note that we used both MoCA and MMSE in this study. There is no consensus as to which tool (MoCA or MMSE) is more accurate in detecting cognitive decline (Jiang et al., 2018). We used both MoCA and MMSE because the MoCA is more sensitive for early detection while the MMSE test is more appropriate in discriminating between moderate and severe stages of AD (Trzepacz et al., 2015). Hence, MoCA and MMSE are complementary for cognitive tests and both were adopted in this study.

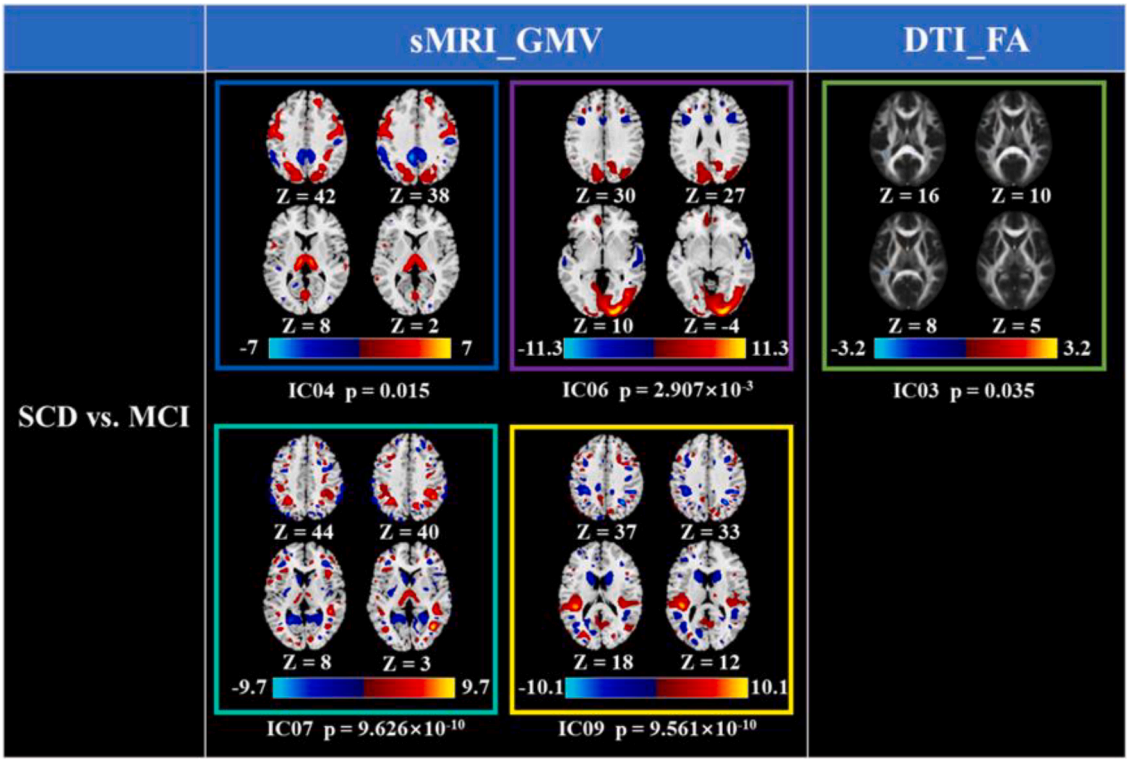

Fig. 4. Main group-discriminative ICs between SCD and MCI patients. GMV and FA were shown in coronal brain maps in terms of z-scores (positive: red, negative: blue; a threshold at $|Z| \geq 2$ was set for visualizing brain regions with large GMV or FA values). Those listed p-values were obtained by post-hoc Tukey-Kramer test between SCD and MCI. (For interpretation of the references to color in this figure legend, the reader is referred to the web version of this article.)

Table 2
Correlations between mixing coefficients of GM and FA.

Index of ICs	**01**	**02**	**03**	**04**	**05**
p value	*7.960 × 10^{-15}	*1.090 × 10^{-7}	*1.696 × 10^{-7}	*6.014 × 10^{-6}	*2.800 × 10^{-5}
Corr. coef	0.481	0.340	0.335	0.292	0.271
Index of ICs	**06**	**07**	**08**	**09**	**10**
p value	*3.993 × 10^{-5}	*5.899 × 10^{-5}	*1.428 × 10^{-4}	*3.365 × 10^{-4}	*1.843 × 10^{-3}
Corr. coef	0.266	0.261	0.247	0.233	0.203
Index of ICs	**11**	**12**	**13**	**14**	**15**
p value	0.013	0.045	0.066	0.091	0.170
Corr. coef	0.162	0.132	0.121	0.111	0.090

Note:The p values with asterisk (*) passed Bonferroni multiple comparisons ($p < 3.333 \times 10^{-3}$)

MoCA was developed by Nasreddine and collaborators (Nasreddine et al., 2005) and has been shown as a tracking tool with a high ability to discriminate normal cognitive function, MCI and early onset dementia. Their results revealed "a cutoff of 26 (scores of 25 or below indicate impairment) yielded the best balance between sensitivity and specificity for the MCI and AD groups", "while separating patients with MCI from those with AD will still rely on clinical judgment, particularly in assessing whether the patient has functional impairment" (Nasreddine et al., 2005). So, the cut-off score for MOCA was not provided as a range of values for MMSE.

4.1.3. FA as the DTI features

When performing mCCA-jICA, we only computed FA, not other features, from DTI because of the following two reasons. First, FA is much more popularly used than MD/AD/RD in the researches of SCD/MCI/AD. Actually, some studies have found multiple DTI indices (FA/MD/AD/RD) can detect the abnormal WM fibers in AD (Kantarci et al., 2017; Gyebnár et al., 2018). Among these indices, FA represents the degree of anisotropy of water molecules and is much more commonly used to characterize the changes at the microstructural level in pathologic processes of MCI/AD (Kantarci, 2014; Ezzati et al., 2016; Evin et al., 2020). Second, most of previous studies about multimodal fusion used FA as DTI features. For example, Ouyang *et al.* have already used FA and GMV for the mCCA-jICA fusion analysis of AD diseases (Ouyang et al., 2015). In multimodal fusion studies of other neurogenerative diseases or mental disorders (such as depression and schizophrenia), FA is also much more frequently used than other indices (Sui et al., 2011; Sui et al., 2013a; Sui et al., 2013b; Wang et al., 2019; Tang et al., 2020). Therefore, FA was chosen for fusion analysis in this study because it is easy to compare our results with previous findings (related to AD or related multimodal MRI fusion). Of course, we agree that, it is definitely possible to compute MD/AD/RD for fusion analysis, which may lead to new findings.

4.1.4. Effect of smoothing

Before performing mCCA-jICA methods on the features, smoothing is an essential step in preprocessing of MRI data. In this study, GM and WM images were smoothed using an 8-mm FWHM Gaussian kernel, which was recommended and widely used in literature. In general, a large kernel will blur the images and reduce the spatial resolution, while a small kernel may not be able to satisfactorily suppress noise. A previous study on fMRI activation used extensive simulations and real-data to prove that, an 8-mm FWHM Gaussian kernel should be optimal (Mikl et al., 2008). However, there is no any in-depth research concerning the effects of smoothing on fusion of sMRI and DTI. We carefully checked published papers using mCCA-jICA and found almost all these studies used an 8-mm FWHM Gaussian kernel. So, we also followed this setting to smooth data. It will be an interesting study to investigate the effects of smoothing on the results of multimodal MRI fusion, but it is outside the

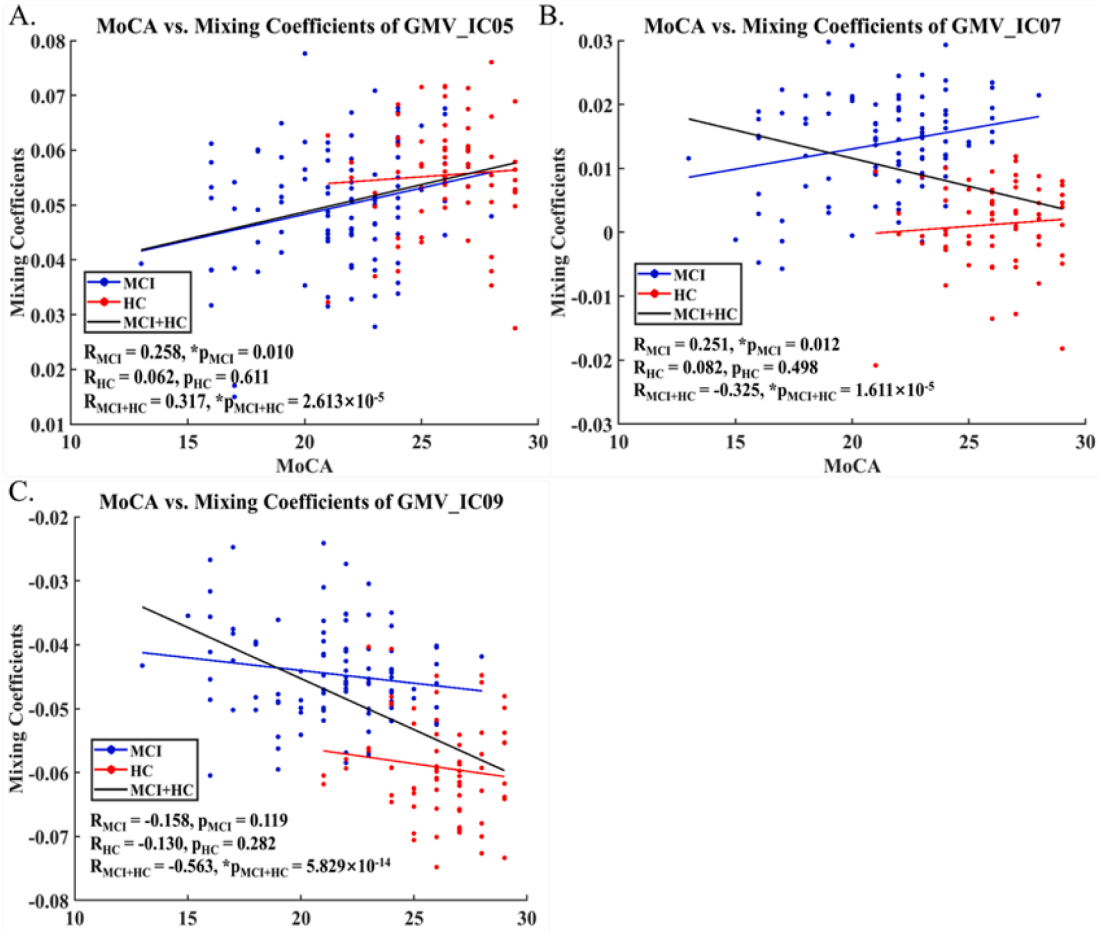

Fig. 5. Correlations between MoCA and mixing coefficients of group-discriminative ICs between HCs and MCI patients. The p values with asterisk (*) passed FDR-corrected threshold of 0.05. A. GMV_IC05. B. GMV_IC07. C. GMV_IC09.

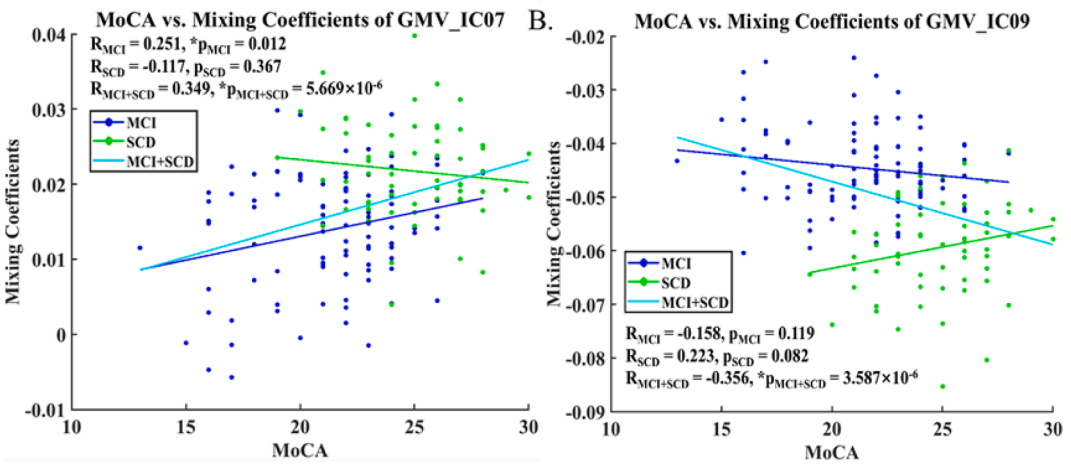

Fig. 6. Correlations between MoCA and mixing coefficients of group-discriminative ICs between SCD and MCI patients. The p values with asterisk (*) passed FDR-corrected threshold of 0.05. A. GMV_IC07. B. GMV_IC09.

scope of this work.

4.1.5. Dimension reduction

Because dimension reduction was used for GMV and FA separately, it is true that the dimensionalities of GMV and FA were different after dimension reduction. In this study, after dimension reduction (achieved by SVD), the number of GMV features was 1,454,255, while the number of FA features was 58,919. From a methodological point of view, different numbers of features will not affect the results of mCCA-jICA largely. First, mCCA will not be influenced by different numbers of features. The original CCA is naturally developed to deal with two variables with different dimensionalities, because it uses two weighting vectors to multiply two matrices of two variables for the calculation of the correlation of these two variables. Second, jICA will not be largely

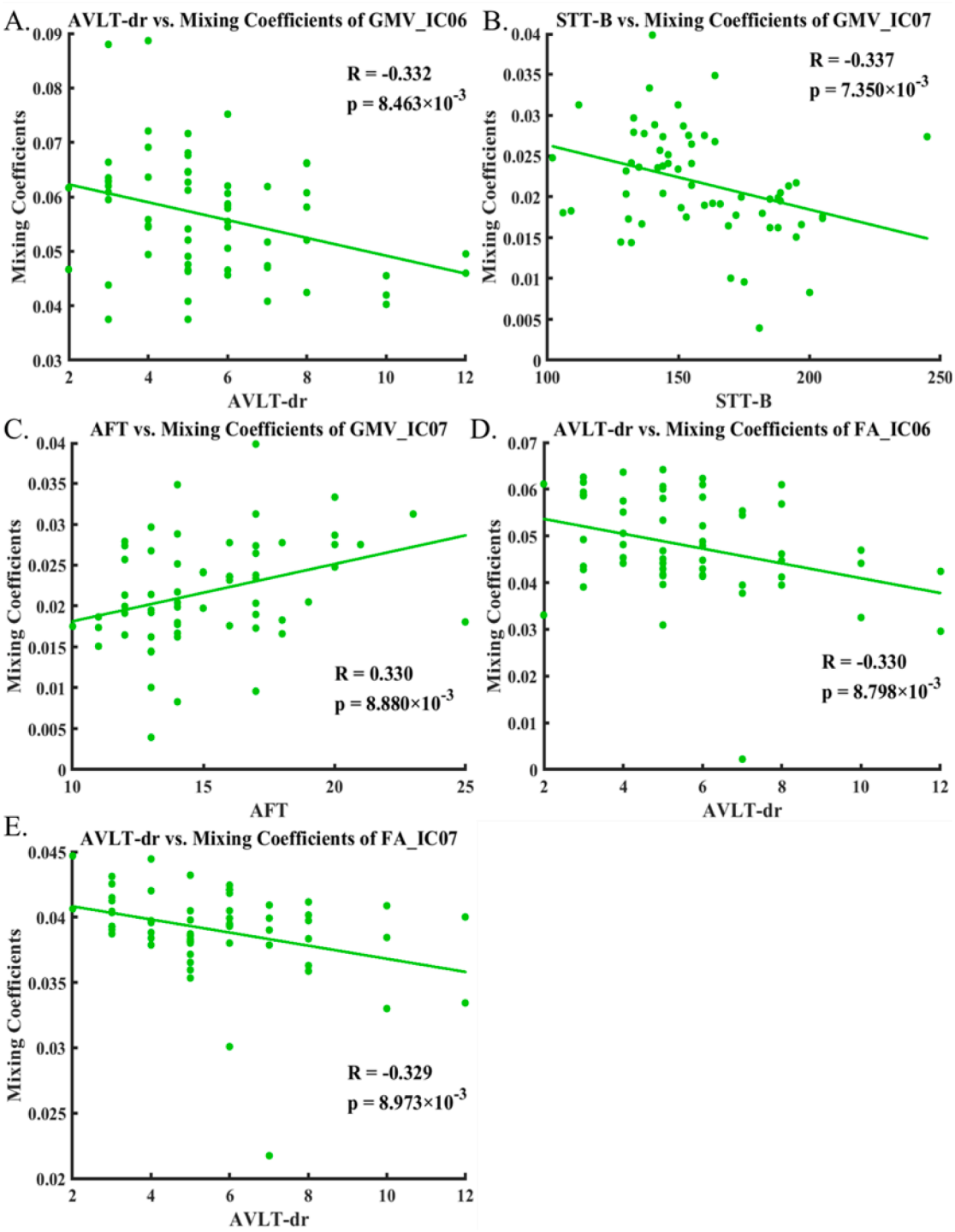

Fig. 7. Correlations between mixing coefficients in SCD patients and measurements of cognitive tests. A. Correlation between AVLT-dr and mixing coefficients of GMV IC06. B. Correlation between STT-B and mixing coefficients of GMV_IC07. C. Correlation between AFT and mixing coefficients of GMV_IC07. D. Correlation between AVLT-dr and mixing coefficients of FA_IC06. E. Correlation between AVLT-dr and mixing coefficients of FA_IC07.

affected by the dimensionalities. jICA works on the concatenated matrix of two modalities and the decomposed components are independent with each other, which means the variable of either modality (GMV or FA) in the decomposed component is independent with each other. Therefore, we believe the results are not largely affected by dimension reduction.

4.1.6. Explanation on FA results

In the following, we explain why the fusion analysis did not find many useful FA components as previous studies did. From a methodological point of view, the disagreement between our results (fewer FA results) and the results in literature is mainly due to the new mCCA-jICA method, which is a multivariate decomposition method used for multimodal data. First, unlike traditional unimodal analysis used literature, this study used a multimodal fusion method, mCCA-jICA, to discover covariant GM-WM components. It means that, the FA components we identified in this study were all covaried with GMV components, while those FA components found in other studies were not necessarily

corelated with WM. Second, because the jICA method decomposes DTI images into a series of ICs, which may be overlapped with each other, an IC with a group difference could overlap another common IC to a large extent. In such a case, traditional univariate analysis, which does not consider possible mixture of multiple components for one voxel, and ICA-like multivariate analysis, which believes the intensity of one voxel can be contributed by difference sources/components, could have largely different results. Actually, some other studies using mCCA-jICA also reported the difference between the results of multimodal/multivariate analysis and unimodal/univariate analysis and provided possible explanations (Kim et al., 2015). Actually, some previous studies have yielded inconsistent FA results in SCD and the abnormalities mainly occurred in the medial temporal lobe and the longitudinal fasciculi, corpus callosum, uncinated fasciculi, while some other studies revealed no significant changes (Selnes et al., 2012; Wang et al., 2020). One of the possible reasons for the inconsistency may be the heterogeneity of the disease and different inclusion criteria.

4.2. Covariation of GM and FA in SCD

For SCD and HC groups, GM_IC7 and FA_IC7 were joint-discriminative components, which suggests the brain's structural abnormalities mainly in bilateral middle temporal gyrus, precentral gyrus, superior frontal gyrus, postcentral gyrus, middle frontal gyrus, calcarine sulcus and superior parietal lobule in GM, and the anterior thalamic radiation and superior longitudinal fasciculus in WM. The anterior thalamic radiation connects the anterior and medial regions of the thalamus to the frontal lobe, and the superior longitudinal fasciculus projects from the frontal lobe to the temporal, parietal, and occipital lobes. Of note, the identified regions of GM and WM are anatomically connected. These identified regions in the present study were consistent with previous findings. For example, Risacher *et al.* (Risacher et al., 2017) found that total scores in the preadjusted smell identification test were significantly correlated with tau deposition in regions including the bilateral middle temporal gyri and precentral gyri, as well as the bilateral superior, middle, and inferior frontal gyri in SCD patients. The middle temporal gyrus is an important part of default mode network (DMN) (Xu et al., 2015), which plays an critical role in cognitive processing. Matias-Guiu *et al.* (Matías-Guiu et al., 2017) found that the metabolism of the middle temporal gyrus was correlated with the Boston naming test scores in SCD. Interestingly, we found the mixing coefficient of GM_IC7 was significantly correlated with AFT, which serves as a measure of the language capability like Boston naming test scores. The precentral gyrus and postcentral gyrus are important parts of the sensorimotor network, which plays a key role in the analysis of information (Flanagan et al., 2013). Atrophy of the precentral gyrus has been reported in SCD patients (Hafkemeijer et al., 2013). Superior frontal gyrus and middle frontal gyrus are involved the frontal network, which is known to participate in the regulation of memory and language functions and executive function (Allen et al., 2011). The calcarine sulcus is an important part of visual network. The abnormalities of the visual cortex resulted in cognitive deficits in AD, and the underlying pathological mechanism may be the formation of amyloid plaques and neurofibrillary tangles (Li et al., 2015). As a risk state of AD, SCD has been reported to have increased connectivity in visual network (Lista et al., 2015). The superior parietal lobe is involved in the attentional network. Previous research revealed more limited subsequent memory effects on the regions including superior parietal lobe in SCD, suggesting brain functional reorganization during memory tasks (Wang et al., 2020). Taken together, the covariate changes in GM were emerged in a wide range of networks, but all the affected regions were involved in cognitive processing.

Further, we found the abnormalities in WM integrity of the superior longitudinal fasciculus in SCD patients, which was consistent with findings from previous reports (Brueggen et al., 2019; Ohlhauser et al., 2019; Luo et al., 2020). For example, a previous study (Ohlhauser et al., 2019) found that the SCD group exhibited a significant correlation between executivefunction and FA in the anterior thalamic radiation, superior longitudinal fasciculus, corticospinal tract, corpus callosum, hippocampi, forceps major, and forceps minor. Also, the mixing coefficient of GM_IC7 was significantly correlated with AVLT-dr. The AVLT-dr test holds the potential to be the best neuropsychological assessment for the identification of AD at an early state and for the prediction of the conversion to AD (Chen et al., 2000; Tierney et al., 2005). Episodic memory is the first cognitive domain affected along the AD continuum, for which AVLT is considered to be one of the best tests (Simard and van Reekum, 1999). To conclude, these results indicated the covariate abnormalities of GM and WM may be contribute to the cognitive function changes in SCD.

4.3. Covariation of GM and FA in MCI

In terms of group differences between MCI and HC, the covariant abnormalities occurred in bilateral meddle temporal gyrus, caudate nucleus and fusiform in GM and forceps minor and bilateral anterior thalamic radiation in WM. The forceps minor is the anterior part of corpus callosum and connects the bilateral prefrontal cortex, and the anterior thalamic radiation connects the anterior and medial regions of the thalamus to the frontal lobe. The identified regions of GM and WM affecting in MCI did not show anatomical connectivity. The middle temporal gyrus is an important part of DMN as aforementioned. The caudate nucleus is involved in working and learning memory, of which the atrophy deteriorates progressively in AD (Sun et al., 2016). Fusiform is well known to be involved in facial cognition, and there were widespread alterations in its connectivity during a face-matching task in MCI (Bokde, 2006). Moreover, the *meta*-analyses demonstrated abnormal activity of fusiform either at resting state or in a task (Li et al., 2015; Pan et al., 2017). The forceps minor is within the structural network that is associated with the functional DMN (Luo et al., 2012) and involved in cognitive dysfunction (Mamiya et al., 2018). Previous studies found abnormalities in the forceps minor were related to cognitive function scores in MCI (Grambaite et al., 2010; Luo et al., 2020). Abnormal WM integrity occurred in anterior thalamic radiation which is involved in cognitive function such as working memory and executive function (Liu et al., 2017). The identified regions with WM alterations were overlapped with those of a recent study (Luo et al., 2020) which demonstrated disrupted WM integrity in the anterior thalamic radiation, corticospinal tract, cingulate gyrus, the cingulum of the hippocampus, forceps minor, forceps major, and inferior fronto-occipital fasciculus. Although these affected regions seem to be anatomically discrete, they all play important roles in cognition. Thus, we believed that the observed covariation of GM and WM might account for changes in cognitive function.

In addition, no significant group differences in GM-WM covariation could be found between MCI and SCD, indicating that the progress from SCD to MCI does not involve covariant GM-WM changes.

To sum up, the covariation of GM and WM in the present study highlighted the interaction between GM regions and the WM that connects them. The coordination of different brain regions plays a critical role in the cognitive performance. Recently developed methods for the analyses of structural imaging could identify the network changes which is beyond the primary brain disruption (Karnath et al., 2018). Even when the contemporary tractography methods were applied in historic cases, the result showed disconnection extended to distant areas which connected to the lesion (Thiebaut de Schotten et al., 2015). The WM disconnection map might help to assess the changes of connectivity between the altered WM integrity and distant GM regions including the cortices and deep gray nuclei, and predict the cognitive alteration (Kuceyeski et al., 2013; Zayed et al., 2020). Our future studies will focus on the alteration of the connectivity between WM and GM, and provide objective evidences for the early diagnosis and prediction of the cognitive decline of the disease.

5. Conclusion

The present study used a multimodal fusion analysis method, mCCA-jICA, to fuse sMRI and DTI data of three groups (HC, SCD, and MCI), with the aim to discover covariant alterations of the brain morphology in SCD and MCI. We identified a set of covariant GM-WM abnormalities of SCD and MCI in cognition-related brain regions, and these covariant GM-WM abnormalities were significantly correlated with cognitive scores in SCD. Our results suggest that multimodal fusion analysis allows for a more comprehensive understanding of the underlying relationships among different MRI modalities in predementia stages of AD, and the study can improve our knowledge regarding the neuropathological mechanism of the disease.

CRediT authorship contribution statement

Lingyan Liang: Writing – original draft, Writing – review & editing. **Zaili Chen:** Formal analysis, Writing – review & editing, Visualization. **Yichen Wei:** Formal analysis, Resources, Visualization. **Fei Tang:** Software, Writing – original draft. **Xiucheng Nong:** Resources. **Chong Li:** Resources. **Bihan Yu:** Resources. **Gaoxiong Duan:** Formal analysis. **Jiahui Su:** Resources. **Wei Mai:** Resources. **Lihua Zhao:** Investigation, Resources. **Zhiguo Zhang:** Data curation, Methodology, Validation. **Demao Deng:** Conceptualization, Project administration, Supervision.

Declaration of Competing Interest

The authors declare that they have no known competing financial interests or personal relationships that could have appeared to influence the work reported in this paper.

Acknowledgements

We thank all the patients who participated in the study, and their families.

Funding

This work was supported by the National Natural Science Foundation of China [grant numbers 81760886, 81871443, 82060315 and 82102032]; the Science and Technology Plan of Guangxi [Gui, grant number 14124004-1-27]; the Guangxi Natural Science Foundation [grant number 2016GXNSFAA380086]; the Natural Science Foundation of Guangdong Province [grant number 2021A1515011152]; the Shenzhen Peacock Plan [grant number KQTD20160531122051497]; the Science, Technology and Innovation Commission of Shenzhen Municipality Technology Fund [grant number 2021SHIBS0003, KCXFZ20201221173400001].

Appendix A. Supplementary data

Supplementary data to this article can be found online at https://doi.org/10.1016/j.nicl.2021.102874.

References

Albert, M.S., DeKosky, S.T., Dickson, D., Dubois, B., Feldman, H.H., Fox, N.C., Gamst, A., Holtzman, D.M., Jagust, W.J., Petersen, R.C., Snyder, P.J., Carrillo, M.C., Thies, B., Phelps, C.H., 2011. The diagnosis of mild cognitive impairment due to Alzheimer's disease: recommendations from the National Institute on Aging-Alzheimer's Association workgroups on diagnostic guidelines for Alzheimer's disease. Alzheimers Dement 7 (3), 270–279.

Allen, E.A., Erhardt, E.B., Damaraju, E., Gruner, W., Segall, J.M., Silva, R.F., Havlicek, M., Rachakonda, S., Fries, J., Kalyanam, R., Michael, A.M., Caprihan, A., Turner, J.A., Eichele, T., Adelsheim, S., Bryan, A.D., Bustillo, J., Clark, V.P., Feldstein Ewing, S.W., Filbey, F., Ford, C.C., Hutchison, K., Jung, R.E., Kiehl, K.A., Kodituwakku, P., Komesu, Y.M., Mayer, A.R., Pearlson, G.D., Phillips, J.P., Sadek, J. R., Stevens, M., Teuscher, U., Thoma, R.J., Calhoun, V.D., 2011. A Baseline for the Multivariate Comparison of Resting-State Networks. Front Syst Neurosci 5. https://doi.org/10.3389/fnsys.2011.00002.

Ashburner, J., 2007. A fast diffeomorphic image registration algorithm. Neuroimage 38 (1), 95–113.

Brueggen, K., Dyrba, M., Cardenas-Blanco, A., Schneider, A., Fliessbach, K., Buerger, K., Janowitz, D., Peters, O., Menne, F., Priller, J., Spruth, E., Wiltfang, J., Vukovich, R., Laske, C., Buchmann, M., Wagner, M., Röske, S., Spottke, A., Rudolph, J., Metzger, C. D., Kilimann, I., Dobisch, L., Düzel, E., Jessen, F., Teipel, S.J., 2019. Structural integrity in subjective cognitive decline, mild cognitive impairment and Alzheimer's disease based on multicenter diffusion tensor imaging. J Neurol 266 (10), 2465–2474.

Calhoun, V.D., Adali, T., 2008. Feature-based fusion of medical imaging data. IEEE Trans Inf Technol Biomed 13, 711–720.

Calhoun, V.D., Sui, J., 2016. Multimodal fusion of brain imaging data: A key to finding the missing link (s) in complex mental illness. Biol Psychiatry Cogn Neurosci Neuroimaging 1, 230–244.

Chen, P., Ratcliff, G., Belle, S.H., Cauley, J.A., DeKosky, S.T., Ganguli, M., 2000. Cognitive tests that best discriminate between presymptomatic AD and those who remain nondemented. Neurology 55 (12), 1847–1853.

Edmonds, E.C., Delano-Wood, L., Galasko, D.R., Salmon, D.P., Bondi, M.W., Brandt, J., 2015. Subtle cognitive decline and biomarker staging in preclinical Alzheimer's disease. J Alzheimers Dis 47 (1), 231–242.

Bokde, A.L.W., Lopez-Bayo, P., Meindl, T., Pechler, S., Born, C., Faltraco, F., Teipel, S.J., Möller, H.-J., Hampel, H., 2006. Functional connectivity of the fusiform gyrus during a face-matching task in subjects with mild cognitive impairment. Brain 5, 1113–1124.

Evin GK, Harı E, Bayram A, *et al.* Fractional anisotropy changes in the fornix and cingulum tracts in Alzheimer's disease continuum. Anatomy Int J Expt C 2020;14.

Ezzati, A., Katz, M.J., Lipton, M.L., Zimmerman, M.E., Lipton, R.B., 2016. Hippocampal volume and cingulum bundle fractional anisotropy are independently associated with verbal memory in older adults. Brain Imaging Behav 10 (3), 652–659.

Flanagan, K.J., Copland, D.A., Chenery, H.J., Byrne, G.J., Angwin, A.J., 2013. Alzheimer's disease is associated with distinctive semantic feature loss. Neuropsychologia 51 (10), 2016–2025.

Folstein, M.F., Folstein, S.E., McHugh, P.R., 1975. "Mini-mental state": a practical method for grading the cognitive state of patients for the clinician. J Psychiatr Res 12 (3), 189–198.

Grambaite, R., Stenset, V., Reinvang, I., Walhovd, K.B., Fjell, A.M., Fladby, T., 2010. White matter diffusivity predicts memory in patients with subjective and mild cognitive impairment and normal CSF total tau levels. J Int Neuropsychol Soc 16 (1), 58–69.

Gyebnár, G., Szabó, Á., Sirály, E., Fodor, Z., Sákovics, A., Salacz, P., Hidasi, Z., Csibri, É., Rudas, G., Kozák, L.R., Csukly, G., 2018. What can DTI tell about early cognitive impairment?–Differentiation between MCI subtypes and healthy controls by diffusion tensor imaging. Psychiatry Res Neuroimaging 272, 46–57.

Hafkemeijer, A., Altmann-Schneider, I., Oleksik, A.M., van de Wiel, L., Middelkoop, H.A. M., van Buchem, M.A., van der Grond, J., Rombouts, S.A.R.B., 2013. Increased Functional Connectivity and Brain Atrophy in Elderly with Subjective Memory Complaints. Brain Connect 3 (4), 353–362.

Jessen, F., Amariglio, R.E., Buckley, R.F., van der Flier, W.M., Han, Y., Molinuevo, J.L., Rabin, L., Rentz, D.M., Rodriguez-Gomez, O., Saykin, A.J., Sikkes, S.A.M., Smart, C. M., Wolfsgruber, S., Wagner, M., 2020. The characterisation of subjective cognitive decline. Lancet Neurol 19 (3), 271–278.

Jessen, F., Amariglio, R.E., Boxtel, M., Breteler, M., Ceccaldi, M., Chételat, G., Dubois, B., Dufouil, C., Ellis, K.A., Flier, W.M., Glodzik, L., Harten, A.C., Leon, M.J., McHugh, P., Mielke, M.M., Molinuevo, J.L., Mosconi, L., Osorio, R.S., Perrotin, A., Petersen, R.C., Rabin, L.A., Rami, L., Reisberg, B., Rentz, D.M., Sachdev, P.S., Sayette, V., Saykin, A. J., Scheltens, P., Shulman, M.B., Slavin, M.J., Sperling, R.A., Stewart, R., Uspenskaya, O., Vellas, B., Visser, P.J., Wagner, M., 2014. A conceptual framework for research on subjective cognitive decline in preclinical Alzheimer's disease. Alzheimers Dement 10 (6), 844–852.

Jiang, L., Sui, D., Qiao, K., Dong, H.-M., Chen, L., Han, Y., 2018. Impaired functional criticality of human brain during Alzheimer's disease progression. Sci Rep 8, 1–11.

Kantarci, K., 2014. Fractional anisotropy of the fornix and hippocampal atrophy in Alzheimer's disease. Front Aging Neurosci 6, 316.

Kantarci, K., Murray, M.E., Schwarz, C.G., Reid, R.I., Przybelski, S.A., Lesnick, T., Zuk, S. M., Raman, M.R., Senjem, M.L., Gunter, J.L., Boeve, B.F., Knopman, D.S., Parisi, J.E., Petersen, R.C., Jack, C.R., Dickson, D.W., 2017. White-matter integrity on DTI and the pathologic staging of Alzheimer's disease. Neurobiol aging 56, 172–179.

Karnath, H.-O., Sperber, C., Rorden, C., 2018. Mapping human brain lesions and their functional consequences. Neuroimage 165, 180–189.

Kim, S.-G., Jung, W.H., Kim, S.N., Jang, J.H., Kwon, J.S., Soriano-Mas, C., 2015. Alterations of gray and white matter networks in patients with obsessive-compulsive disorder: a multimodal fusion analysis of structural MRI and DTI using mCCA+ jICA. PLoS One 10 (6), e0127118. https://doi.org/10.1371/journal.pone.0127118.

Kuceyeski, A., Maruta, J., Relkin, N., Raj, A., 2013. The Network Modification (NeMo) Tool: elucidating the effect of white matter integrity changes on cortical and subcortical structural connectivity. Brain Connect 3 (5), 451–463.

Lazarou, I., Nikolopoulos, S., Dimitriadis, S.I., (Yiannis) Kompatsiaris, I., Spilioti, M., Tsolaki, M., 2019. Is brain connectome research the future frontier for subjective cognitive decline? A systematic review. Clin Neurophysiol 130 (10), 1762–1780.

Lerman-Sinkoff, D.B., Sui, J., Rachakonda, S., Kandala, S., Calhoun, V.D., Barch, D.M., 2017. Multimodal neural correlates of cognitive control in the Human Connectome Project. Neuroimage 163, 41–54.

Li, H.J., Hou, X.H., Liu, H.H., Yue, C.L., He, Y., Zuo, X.N., 2015. Toward Systems Neuroscience in Mild Cognitive Impairment and Alzheimer's Disease: A Meta-Analysis of 75 fMRI Studies. Hum Brain Mapp 36 (3), 1217–1232.
Li, Y.O., Adalı, T., Calhoun, V.D., 2007. Estimating the number of independent components for functional magnetic resonance imaging data. Hum Brain Mapp 28 (11), 1251–1266.
Lista, S., Molinuevo, J.L., Cavedo, E., Rami, L., Amouyel, P., Teipel, S.J., Garaci, F., Toschi, N., Habert, M.-O., Blennow, K., Zetterberg, H., O'Bryant, S.E., Johnson, L., Galluzzi, S., Bokde, A.L.W., Broich, K., Herholz, K., Bakardjian, H., Dubois, B., Jessen, F., Carrillo, M.C., Aisen, P.S., Hampel, H., Tales, A., Jessen, F., Butler, C., Wilcock, G., Phillips, J., Bayer, T., 2015. Evolving evidence for the value of neuroimaging methods and biological markers in subjects categorized with subjective cognitive decline. J Alzheimers Dis 48 (s1), S171–S191.
Liu, J., Liang, P., Yin, L., Shu, N.i., Zhao, T., Xing, Y.i., Li, F., Zhao, Z., Li, K., Han, Y., Liu, Y., 2017. White matter abnormalities in two different subtypes of amnestic mild cognitive impairment. PLoS One 12 (1), e0170185. https://doi.org/10.1371/journal.pone.0170185.
López-Sanz, D., Bruña, R., Garcés, P., Martín-Buro, M.C., Walter, S., Delgado, M.L., Montenegro, M., López Higes, R., Marcos, A., Maestú, F., 2017. Functional connectivity disruption in subjective cognitive decline and mild cognitive impairment: a common pattern of alterations. Front Aging Neurosci 9. https://doi.org/10.3389/fnagi.2017.00109.
Lottman, K.K., White, D.M., Kraguljac, N.V., et al., 2018. Four-way multimodal fusion of 7 T imaging data using an m CCA+ j ICA model in first-episode schizophrenia. Hum Brain Mapp 39, 1475–1488.
Luo, C., Li, M., Qin, R., Chen, H., Yang, D., Huang, L., Liu, R., Xu, Y., Bai, F., Zhao, H., 2020. White matter microstructural damage as an early sign of subjective cognitive decline. Front Aging Neurosci 11. https://doi.org/10.3389/fnagi.2019.00378.
Luo, L.i., Xu, L., Jung, R., Pearlson, G., Adali, T., Calhoun, V.D., 2012. Constrained source-based morphometry identifies structural networks associated with default mode network. Brain Connect 2 (1), 33–43.
Mamiya, P.C., Richards, T.L., Kuhl, P.K., 2018. Right forceps minor and anterior thalamic radiation predict executive function skills in young bilingual adults. Front Psychol 9.
Matías-Guiu, J.A., Cabrera-Martín, M.N., Valles-Salgado, M., Pérez-Pérez, A., Rognoni, T., Moreno-Ramos, T., Carreras, J.L., Matías-Guiu, J., 2017. Neural Basis of Cognitive Assessment in Alzheimer Disease, Amnestic Mild Cognitive Impairment, and Subjective Memory Complaints. Am J Geriatr Psychiatry 25 (7), 730–740.
Mikl, M., Mareček, R., Hluštík, P., Pavlicová, M., Drastich, A., Chlebus, P., Brázdil, M., Krupa, P., 2008. Effects of spatial smoothing on fMRI group inferences. Magn Reson Imaging 26 (4), 490–503.
Nasreddine, Z.S., Phillips, N.A., Valérie Bédirian, Charbonneau, S., Chertkow, H., 2005. The montreal cognitive assessment, moca: a brief screening tool for mild cognitive impairment. J Am Geriatr Soc 53 (4), 695–699.
Ohlhauser, L., Parker, A.F., Smart, C.M., Gawryluk, J.R., 2019. Initiative AsDN. White matter and its relationship with cognition in subjective cognitive decline. Alzheimers Dement (Amst) 11 (1), 28–35.
Ouyang, X., Chen, K., Yao, L., Hu, B., Wu, X., Ye, Q., Guo, X., 2015. Simultaneous changes in gray matter volume and white matter fractional anisotropy in Alzheimer's disease revealed by multimodal CCA and joint ICA. Neuroscience 301, 553–562.
Pan, P., Zhu, L., Yu, T., Shi, H., Zhang, B., Qin, R., Zhu, X., Qian, L., Zhao, H., Zhou, H., Xu, Y., 2017. Aberrant spontaneous low-frequency brain activity in amnestic mild cognitive impairment: a meta-analysis of resting-state fMRI studies. Ageing Res Rev 35, 12–21.
Rajapakse, J.C., Giedd, J.N., Rapoport, J.L., 1997. Statistical approach to segmentation of single-channel cerebral MR images. IEEE Trans Med Imaging 16 (2), 176–186.
Risacher, S.L., Tallman, E.F., West, J.D., Yoder, K.K., Hutchins, G.D., Fletcher, J.W., Gao, S., Kareken, D.A., Farlow, M.R., Apostolova, L.G., Saykin, A.J., 2017. Olfactory identification in subjective cognitive decline and mild cognitive impairment: association with tau but not amyloid positron emission tomography. Alzheimers Dement (Amst) 9 (1), 57–66.
Selnes, P., Fjell, A.M., Gjerstad, L., Bjørnerud, A., Wallin, A., Due-Tønnessen, P., Grambaite, R., Stenset, V., Fladby, T., 2012. White matter imaging changes in subjective and mild cognitive impairment. Alzheimers Dement 8 (5S). https://doi.org/10.1016/j.jalz.2011.07.001.
Simard, M., van Reekum, R., 1999. Memory assessment in studies of cognition-enhancing drugs for Alzheimer's disease. Drugs Aging 14 (3), 197–230.
Smith, S.M., Jenkinson, M., Johansen-Berg, H., Rueckert, D., Nichols, T.E., Mackay, C.E., Watkins, K.E., Ciccarelli, O., Cader, M.Z., Matthews, P.M., Behrens, T.E.J., 2006. Tract-based spatial statistics: voxelwise analysis of multi-subject diffusion data. Neuroimage 31 (4), 1487–1505.
Strang, G., 1993. Introduction to linear algebra. Wellesley-Cambridge Press Wellesley, MA.
Sui, J., Huster, R., Yu, Q., Segall, J.M., Calhoun, V.D., 2014. Function–structure associations of the brain: evidence from multimodal connectivity and covariance studies. Neuroimage 102, 11–23.
Sui, J., Pearlson, G., Caprihan, A., Adali, T., Kiehl, K.A., Liu, J., Yamamoto, J., Calhoun, V.D., 2011. Discriminating schizophrenia and bipolar disorder by fusing fMRI and DTI in a multimodal CCA+ joint ICA model. Neuroimage 57 (3), 839–855.
Sui, J., He, H., Yu, Q., et al., 2013a. Combination of resting state fMRI, DTI, and sMRI data to discriminate schizophrenia by N-way MCCA+ jICA. Front Hum Neurosci 7, 235.
Sui, J., He, H., Pearlson, G.D., Adali, T., Kiehl, K.A., Yu, Q., Clark, V.P., Castro, E., White, T., Mueller, B.A., Ho, B.C., Andreasen, N.C., Calhoun, V.D., 2013b. Three-way (N-way) fusion of brain imaging data based on mCCA+ jICA and its application to discriminating schizophrenia. Neuroimage 66, 119–132.
Sun, Y., Dai, Z., Li, Y., Sheng, C., Li, H., Wang, X., Chen, X., He, Y., Han, Y., 2016. Subjective cognitive decline: mapping functional and structural brain changes—a combined resting-state functional and structural MR imaging study. Radiology 281 (1), 185–192.
Tang, F., Yang, H., Li, L., Ji, E., Fu, Z., Zhang, Z., 2020. Fusion analysis of gray matter and white matter in bipolar disorder by multimodal CCA-joint ICA. J Affective Disord 263, 80–88.
Thiebaut de Schotten, M., Dell'Acqua, F., Ratiu, P., Leslie, A., Howells, H., Cabanis, E., Iba-Zizen, M.T., Plaisant, O., Simmons, A., Dronkers, N.F., Corkin, S., Catani, M., 2015. From Phineas Gage and Monsieur Leborgne to HM: revisiting disconnection syndromes. Cerebral Cortex 25 (12), 4812–4827.
Tierney, M.C., Yao, C., Kiss, A., McDowell, I., 2005. Neuropsychological tests accurately predict incident Alzheimer disease after 5 and 10 years. Neurology 64 (11), 1853–1859.
Tohka, J., Zijdenbos, A., Evans, A., 2004. Fast and robust parameter estimation for statistical partial volume models in brain MRI. Neuroimage 23 (1), 84–97.
Trzepacz, P.T., Hochstetler, H., Wang, S., Walker, B., Saykin, A.J., 2015. Relationship between the Montreal Cognitive Assessment and Mini-mental State Examination for assessment of mild cognitive impairment in older adults. BMC Geriatr 15, 1–9.
Tzourio-Mazoyer, N., Landeau, B., Papathanassiou, D., Crivello, F., Etard, O., Delcroix, N., Mazoyer, B., Joliot, M., 2002. Automated anatomical labeling of activations in SPM using a macroscopic anatomical parcellation of the MNI MRI single-subject brain. Neuroimage 15 (1), 273–289.
Wang, X., Zhao, N.a., Shi, J., Wu, Y., Liu, J., Xiao, Q., Hu, J., 2019. Discussion on the Application of Multi-modal Magnetic Resonance Imaging Fusion in Schizophrenia. J Med Syst 43 (5). https://doi.org/10.1007/s10916-019-1215-7.
Wang, X., Huang, W., Su, L.i., Xing, Y., Jessen, F., Sun, Y.u., Shu, N.i., Han, Y., 2020. Neuroimaging advances regarding subjective cognitive decline in preclinical Alzheimer's disease. Mol Neurodegener 15 (1). https://doi.org/10.1186/s13024-020-00395-3.
Wang, Y., West, J.D., Flashman, L.A., Wishart, H.A., Santulli, R.B., Rabin, L.A., Pare, N., Arfanakis, K., Saykin, A.J., 2012. Selective changes in white matter integrity in MCI and older adults with cognitive complaints. Biochim Biophys Acta 1822 (3), 423–430.
Xu, J., Wang, J., Fan, L., et al., 2015. Tractography-based parcellation of the human middle temporal gyrus. Sci Rep 5, 1–13.
Yang, H., Liu, J., Sui, J., Pearlson, G., Calhoun, V.D., 2010. A hybrid machine learning method for fusing fMRI and genetic data: combining both improves classification of schizophrenia. Front Hum Neurosci 4, 192.
Yang, M.H., Yao, Z.F., Hsieh, S., 2019. Multimodal neuroimaging analysis reveals age-associated common and discrete cognitive control constructs. Hum Brain Mapp 40 (9), 2639–2661.
Zayed A, Iturria-Medina Y, Villringer A, Sehm B, Steele CJ. Rapid Quantification of White Matter Disconnection in the Human Brain. 2020 42nd Annual International Conference of the IEEE Engineering in Medicine & Biology Society (EMBC); 2020: IEEE: 1701-1704.